Wavelets and Ridgelets for Biomedical Image Denoising

D. MARY SUGANTHARATHNAM
Assistant Professor
Government College of Engineering, Tirunelveli, TamilNadu, INDIA.
maryvictorin@yahoo.co.in

DR. D. MANIMEGALAI
Professor
National Engineering College
Kovilpatti, TamilNadu, INDIA.
megalai_nec@yahoo.co.in

B. GANAPATHY RAM
P.G. Scholar
Anna University, Tirunelveli Region, TamilNadu, INDIA.
ganathippu@gmail.com

Abstract:- Image de-noising is a key step in the processing of medical images as they are often corrupted by noise in the process of receiving, coding and transmission. In this paper the performance of Discrete Wavelet Transform (DWT) (Bivariate shrinkage), Stationary Wavelet Transform (SWT) (hard thresholding), Dual Tree Complex Wavelet Transform (DTCWT) (Bivariate shrinkage) and Ridgelet Transform (Hard thresholding) for biomedical image de-noising are evaluated and compared in terms of Peak Signal to Noise Ratio (PSNR). The DWT in many applications reaches its limitations such as oscillations of coefficients at a singularity, lack of directional selectivity in higher dimensions, aliasing and consequent shift variance. Therefore SWT and DTCWT, both with their shift invariant property are studied. DTCWT a moderately redundant multi-resolution transform with decimated sub bands runs into two DWT trees (real and imaginary) of real filters producing the real and imaginary parts of the coefficients. A locally adaptive de-noising algorithm using the bivariate shrinkage function is illustrated using both DWT and DTCWT. A simple bivariate shrinkage rule is described to model the statistics of wavelet coefficients of images. The Ridgelet transform was developed over several years to break the limitations of Wavelet Transform and possesses high directional selectivity. Simulations and experimental results demonstrate that the DTCWT outperforms SWT and DWT as well as Ridgelets in denoising biomedical images corrupted by Random noise, Salt and pepper noise and Gaussian noise while SWT outperforms other wavelet techniques and Ridgelets in de-noising biomedical images degraded by Speckle noise and Poisson noise.

Key words: - De-noising, Wavelet, Ridgelet, Bivariate shrinkage, Threshold.

1 Introduction

Digital Image acquisition involves several optical and electronic devices whose imperfections generate noise in the acquired image. Medical image processing is the use of algorithms and procedures for operations such as image enhancement, image compression etc. Several state of the art equipments that produce human organs in digital form used during treatment include X-ray based methods such as radiography, CT(Computed Tomography), MRI(Magnetic resonance Imaging), PET(Positron Emission Tomography)and SPECT(Single Photon Emission computed Tomography) and several methods in optical imaging.

The main problem encountered by medical imaging systems is the distortion of visual signals obtained due to imperfect acquisition and transmission errors. Noise in medical images has two disadvantages. They are (i) degradation of image quality, (ii) obscuring important information required for accurate diagnosis. Thus all medical imaging devices need some de-noising algorithm to enhance the image under consideration and thus help the medical practitioner to make diagnosis quickly and efficiently. The goal of removing various types of noise in biomedical images is to suppress the noise while preserving the integrity of edge and detail information associated with the original image. Medical images are usually represented in low contrast and noise suppression in these images is particularly a difficult task. A trade off between noise reduction and the preservation of actual features has to be made in a way that enhances the diagnostically relevant image content. Multi scale decompositions have shown significant advantages in representation of signals in de-noising.

Wavelet transforms have emerged as a premier tool for image de-noising due to statistically useful properties of wavelet co-efficients. Its energy compaction and multi-resolution properties has made wavelet as a powerful tool in image de-noising. Hence shrinkage methods combined with wavelets is widely used. Though wavelet transforms have been successfully used in many scientific fields such as image de-noising, ridgelets deals effectively with line singularities.

This paper is organized as follows: Section 2 presents the literature review and motivation. In Section 3, the various Multi-resolution transforms are illustrated. The thresholding used in image denoising algorithm is discussed in Section 4.In section 5 the de-noising algorithm using bivariate shrinkage function and the local adaptive image enhancement algorithm is discussed. The experimental results are discussed in Section 6. Finally the conclusions are drawn in Section 7.

2. Literature review and Motivation

Over the last decade abundant interest has been shown in wavelet methods for noise removal in signal and images. Initial efforts included very simple ideas like thresholding of orthogonal wavelet coefficients of the noisy data followed by reconstruction. Later efforts found that substantial improvements in perceptual quality could be obtained by translation invariant methods based on thresholding of an un-decimated wavelet transform [1][20].

Donoho and his co-workers pioneered a wavelet denoising scheme by using soft thresholding and hard thresholding[3]. This approach appears to be a good choice for a number of applications. This is because a wavelet transform can compact the energy of the image only to a small number of large coefficients and the majority of the wavelet coefficients are very small so that they can be set to zero. Donoho's algorithm offers the advantages of smoothness and adaptation. This algorithm exhibits visual artifacts, therefore a translation invariant denoising scheme to suppress such artifacts by averaging over the de-noising signals of all circular shifts is used.

In the literature many image denoising methods have been proposed to remove additive white Gaussian noise only. For example D. L. Donoho and I.M Johnstone proposed denoising images corrupted with additive white Gaussian noise by thresholding the wavelet co-efficients[2][25]. Further removal of additive Gaussian noise in natural images has been implemented by Shan Gai et al. and Shyam Lal et al[13][15].

In addition Nick kingsbury adopted a method for removing additive Gaussian noise from digital images based on statistical modelling of co-efficients[12].H.A. Noubari et al. has introduced optimal thresholding of wavelet co-efficients[21].

Wen-Chien Yen and Ahen-Chuan tai has focussed only on the removal of Speckle noise in ultrasound images and Shuai Xing and Qing Xu has proposed a bivariate shrinkage function for removal of speckle noise in Synthetic Aperture Radar Images(SAR)[14][11].Latha Parthiban and R. Subramanian have implemented the removal of speckle noise in medical images using Contourlets and have proved that it offers much better performance than wavelets[10].

Ling Wang et al. have utilized Multiwavelet multiresolution analysis using co-variance shrink in removing Poisson noise in medical X-ray images[9].S. Kother Mohideen has proved that Complex Wavelet Transform using Neigh Sure shrink algorithm achieves better results than Discrete Wavelet Transform in the removal of additive Gaussian noise[19].

The critically sampled DWT is applied to a wide range of image processing tasks. However its performance is limited because of oscillations of coefficients at singularity, shift variance, aliasing and lack of directional selectivity in higher dimensions .To overcome this shift dependence problem the Dual Tree Complex Wavelet Transform (DTCWT) is used which is nearly shift invariant and is oriented in 2D. The 2D dual tree wavelet transform produces six sub bands at each scale, each of which is strongly oriented at distinct angles [4].

The decimated DWT used in image denoising algorithms has non-redundant orthogonal property. Although the Stationary Wavelet Transform (SWT) reduces this problem substantially, it is computationally expensive[16]. To overcome the limitations of Wavelets in the applications of high dimensions a new system of representation namely Ridgelets is proposed by Candes and Donoho. Ridgelets deals effectively with line or super plane singularities [6]. But images always exhibit edge discontinuities across curves. However at sufficiently fine scales a curved edge is almost straight, so we can use ridgelets to analyse curves in a localized manner at sufficiently fine scales.

This work explores the utility of Wavelets and Ridgelets for denoising medical images corrupted by various types of noises namely, Random noise, Salt and Pepper noise, Gaussian noise, Speckle noise and Poisson noise. A local adaptive estimation of necessary parameters for the bivariate shrinkage function will be described [8]. The performance of the system will be demonstrated on DWT and DTCWT with bivariate shrinkage and some comparisons with the redundant SWT and Ridgelets is given in order to illustrate the effectiveness of a particular technique[7]. A denoising algorithm using locally adaptive bivariate shrinkage function for medical images is implemented with DWT and DTCWT [5][17]. It is a low complexity denoising algorithm using the joint statistics of the wavelet coefficients of medical images. The bivariate shrinkage function models the relationship between the parent and child coefficients located respectively at different scales of multi-resolution decomposition.

The various wavelet techniques are classified according to different medical images on the basis of PSNR. This paper describes the various de-noising techniques such as DWT, SWT, DCWT and Ridgelets degraded by various types of noise and all these methods are compared in terms of PSNR [22]. The quality of de-noised images is determined by calculating the PSNR which is one of the quantitative measures for image quality evaluation.

Existing approaches as stated in the literature mainly is focussed in the removal of white Gaussian noise in natural images [13]. Very few literatures has concentrated in the removal of only a specific type of noise, for example either Speckle noise in Ultrasound images or Poisson noise in medical X-ray images. The idea of comparison of different methodologies can be revealed from [23][24][26].

In this paper the classical problem of removing various types of noise such as Random noise, Salt and Pepper noise, Gaussian noise, Speckle noise and Poisson noise in different medical imaging modalities is addressed[18].The transforms used are Wavelet Transforms like DWT,SWT and DTCWT. Further initial efforts on image denoising based on recently introduced family of transforms, namely Ridgelets has been proposed as alternatives to wavelet representation of image data.

Certain wavelet techniques works excellently for a certain type of original image or degradation while it may not be suitable for other images. Therefore the choice of right wavelet techniques for a particular type of noise is important in a specific imaging modality as it will determine the final result of the images.

Standard Wavelet methods using Bi-variate shrinkage and thresholding is compared with the Ridgelets and the choice of a particular transform for a specific medical imaging modality in the removal of a particular type of noise is justified in terms of PSNR.

3 Methodology

3.1 Wavelet Transform

Wavelets are mathematical functions that analyze data according to scale or resolution. They aid in studying a signal in different windows or at different resolutions. For instance, if the signal is viewed in a large window, gross features can be noticed, but if viewed in a small window, only small features can be noticed. Wavelets provide some advantages over Fourier transforms. For example, they do a good job in approximating signals with sharp spikes or signals having discontinuities. The term “wavelets” is used to refer to a set of orthonormal basis functions generated by dilation and translation of scaling function φ and a mother wavelet ψ. The finite scale multi resolution representation of a discrete function can be called as a discrete wavelet transform. DWT is a fast linear operation on a data vector, whose length is an integer power of 2. This transform is invertible and orthogonal, where the inverse transform expressed as a matrix is the transpose of the transform matrix. The wavelet basis or function, unlike sines and cosines as in Fourier transform, is quite localized in space. But similar to sines and cosines, individual wavelet functions are localized in frequency.

3.2 Discrete Wavelet Transform:

A DWT is any wavelet transform for which the wavelets are discretely sampled. A key advantage it has over Fourier transform is temporal resolution, it captures both frequency and location information. The DWT of image signal produces a non redundant image representation which provides better spatial and spectral localization. The DWT can be interpreted as signal decomposition in a set of independent spatially oriented frequency channels. The signal is passed through two complimentary filters and emerges as two signals, approximations and details. This is called decomposition or analysis. The components can be assembled back into the original signal without loss of information and this is called as reconstruction or synthesis.

$$\text{Forward DWT}: \ a_{jk} = \sum_{t} f(t)\Psi^{*}_{jk}(t) \qquad (1)$$

$$\text{Inverse DWT}: \ f(t) = \sum_{k}\sum_{j} a_{jk}\Psi_{jk}(t) \qquad (2)$$

$$\Psi_{jk}(t) = 2^{j/2}\Psi(2^{j}t - k) \qquad (3)$$

We can construct discrete WT via iterated (octave band) filter bands as shown in Figure 1.

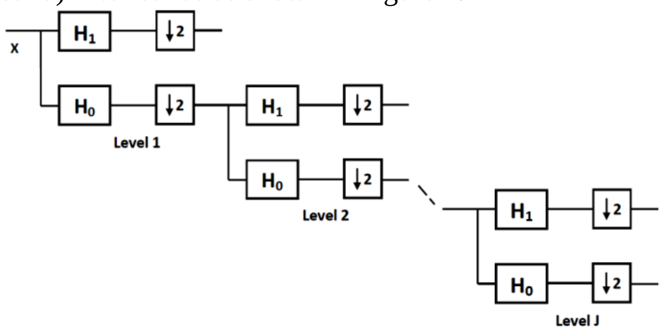

Figure 1. Construction of Wavelet Transform

3.2.1 Analysis Section

For images we use separable WT . First a 1D filter bank is applied to the rows of the image. Then the same transform is applied to the columns of each channel of the result. Therefore 3 high pass channels corresponding to vertical, horizontal and diagonal and one approximation image is obtained. The above procedure can be iteratively applied on the low pass channel. The analysis and synthesis filters are shown in Figure 2 and Figure 3 respectively.

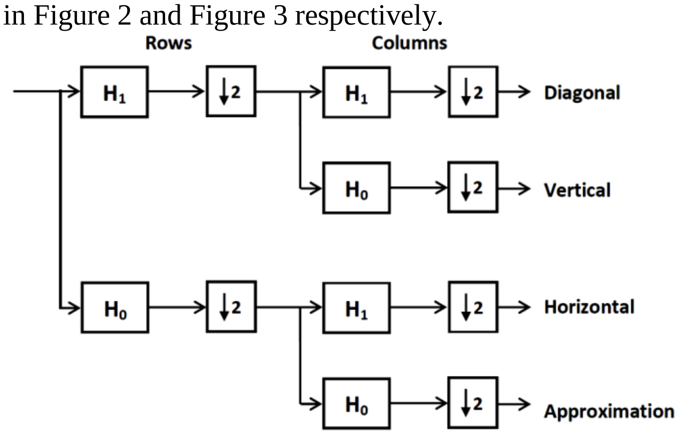

Figure 2. 2D Analysis filter bank

The Discrete wavelet transform of a 2D signal is

$$DWT(m,n) = 2^{-m/2}\sum_{k} S(k)\Psi(2^{-m}k - n) \qquad (4)$$

The DWT uses wavelet filtering and down sampling and it is a reversible process. The wavelets break the signal down into a series of a_j (average coefficients) and d_j (detail coefficients).

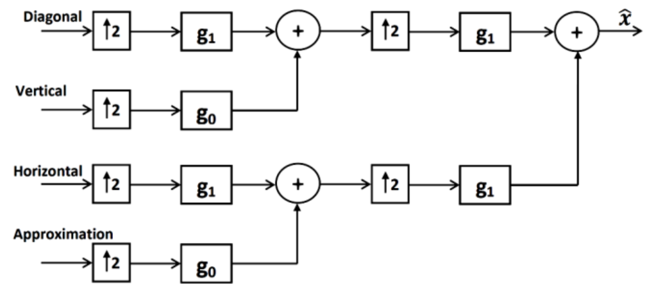

Figure 3. 2D Synthesis filter bank

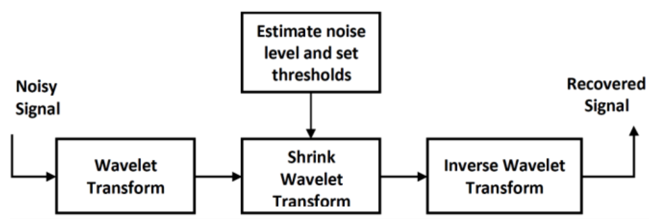

Figure 4. Scheme for Wavelet Denoising

The wavelet model is shown in Figure 4. The steps involve forward DWT and Non linear thresholding followed by Inverse DWT.

3.3 Complex 2-D Dual-tree Wavelet Transform

The dual-tree complex DWT (DT-CDWT) of a signal x is implemented using two critically-sampled DWTs in parallel on the same data, as shown in the Figure 5.

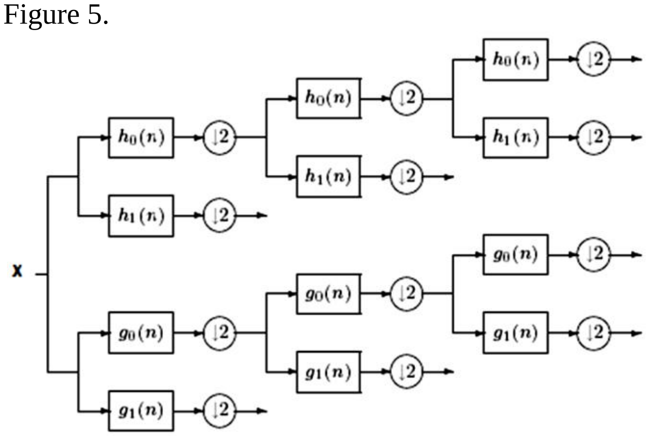

Figure 5. Dual Tree Complex Discrete wavelet Transform

The DTCWT is a Multi resolution transform with decimated sub bands and provides perfect reconstruction at the input. The DTCWT calculates the complex transform of a signal using two separate DWT decompositions .If the filters used in one are specifically designed different from those in the other it is possible for one DWT to produce the real coefficients and the other the imaginary. This redundancy of two provides extra information for analysis but at the expense of extra computational power. It also provides approximate shift invariance yet still allows perfect reconstruction of the signal. The wavelet associated with the upper DWT can be an approximate Hilbert transform of the wavelet associated with the lower DWT. The complex 2D dual tree DWT gives rise to wavelets in six distinct directions one the real part of the complex valued 2D wavelet while the other is the imaginary part.

$\Psi_1(x,y) = \varphi(x)\Psi(y)$ (LH Wavelet) (5)

$\Psi_2(x,y) = \Psi(x)\varphi(y)$ (HL Wavelet) (6)

$\Psi_3(x,y) = \Psi(x)\Psi(y)$ (HH Wavelet) (7)

The two real wavelet transforms use two different sets of filters with each satisfying the perfect reconstruction conditions. The two sets of filters are jointly designed so that the overall transform is approximately analytic.

Let $h_0(n)$ and $h_1(n)$denote the low pass and high pass filter pair for the upper filter bank and let $g_0(n)$ and $g_1(n)$ denote the low pass and high pass filter pair for the lower filter bank. The two real wavelets associated with each of the two real wavelet transforms are denoted as $\Psi_h(t)$ and $\Psi_g(t)$. In addition to satisfying the perfect reconstruction condition the filters are designed so that the complex wavelet $\Psi(t) \coloneqq \Psi_h(t) + j\Psi_g(t)$ is approximately analytic. They are designed such that $\Psi_g(t)$ is approximately the Hilbert transform of $\Psi_h(t)$.

The filters themselves are real and no complex arithmetic is required for the implementation of the dual tree CWT. The dual tree CWT is not a critically sampled transform. It is two times expansive in 1D because the total output data rate is exactly twice the input data rate. To obtain the inverse of DTCWT, the real part and the imaginary part are each inverted, the inverse of each of the two real DWT's are used to obtain two real signals. These two real signals are then averaged to obtain the final output. Finally the original signal can be reconstructed from the real part or the imaginary part alone.

3.4. Overview of Stationary Wavelet Transform (SWT)

The down sampling operation must be suppressed to make it translation invariant and the decomposition is redundant. This is called SWT. Thus the approximation coefficients and the detail coefficients at each level are the same length as the original signal. The high and low pass filters are applied to the data at each level. Decimation is not performed. The filters are modified at each level by padding them with zeros. This transform is computationally more complex. The computational complexity of SWT is O(n^2).The redundant representation makes SWT shift invariant and suitable for application such as de-noising.

In this section the basic principles of the SWT method is presented. In general the Stationary Wavelet Transform method can be portrayed as follows. At each level the data is given to both the high pass and low pass filters so as to produce the two new sequences having same length as the original sequences. For doing this the original data is not decimated. However the filters at each level can be altered by padding zeros with them.

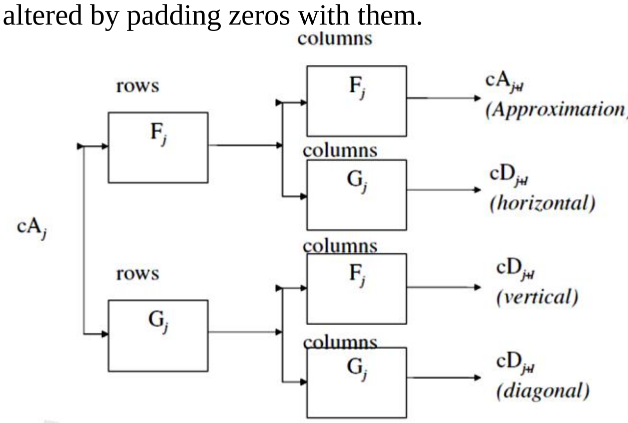

Figure 6. Stationary Wavelet Method

If suppose, a function f(x) is projected at each step j on the subset V_j then the projection is defined by the scalar product $c_{j,k}$ of f(x) with the scaling function $\varphi(x)$ which is dilated and translated.

$$c_{j,k} = \langle f(x), \varphi_{j,k}(x)\rangle \quad (8)$$

$$\varphi_{j,k}(x) = 2^{-j}\varphi(2^{-j}x - k) \quad (9)$$

In equation (9) the term φ(x) denotes the scaling function which is a low pass filter. $c_{j,k}$ is also called a discrete approximation at the resolution 2^j.

If $\varphi(x)$ is the wavelet function, the wavelet coefficients are obtained by

$$w_{j,k} = \langle f(x), 2^{-j}\varphi(2^{-j}x - k)\rangle \quad (10)$$

$w_{j,k}$ is called the discrete detail signal at the resolution 2^j

As the scaling function $\varphi(x)$ has the following property

$$\frac{1}{2}\varphi\left(\frac{x}{2}\right) = \sum_n h(n)\varphi(x-n) \quad (11)$$

$c_{j+1,k}$ can be determined by direct computation from $c_{j,k}$

$$c_{j+1,k} = \sum_n h(n-2k)c_{j,k} \quad (12)$$

$$\frac{1}{2}\varphi\left(\frac{x}{2}\right) = \sum_n g(n)\varphi(x-n) \quad (13)$$

The scalar products $\langle f(x), 2^{-(j+1)}\varphi(2^{-(j+1)}x-k)\rangle$are computed with

$$w_{j+1,k} = \sum_n g(n-2k)c_{j,n} \quad (14)$$

Equations 13 and 14 are the multi resolution algorithm of the traditional DWT. In this transform a down sampling algorithm is used to perform the transformation. That is one out of two points is kept during transformation. Therefore the whole length of the function f(x) will reduce by half after the transformation. This process continues until the length of the function becomes one. However for stationary or redundant transform instead of down sampling an up sampling procedure is carried out before performing filter convolution at each scale. The distance between samples increasing by a factor of two from scale j to the next $c_{j+1,k}$ is obtained by

$$c_{j+1,k} = \sum_l g(l)c_{j,k+}\, 2^j l \quad (15)$$

The discrete wavelet coefficient can be given by

$$w_{j+1,k} = \sum_l h(l)c_{j,k+}\, 2^j l \quad (16)$$

The redundancy of this transform facilitates the identification of salient features in a signal especially for recognizing the noises. In Stationary Wavelet Transform (SWT) instead of down sampling, an up sampling procedure is carried out before we separate the variables x and y of image f(x, y) shown in the following wavelets.

Vertical wavelet (LH): $\varphi^1(x,y) = \varphi(x)\varphi(y)$

Horizontal Wavelet (HL): $\varphi^2(x,y) = \varphi(x)\varphi(y)$

Diagonal Wavelet (HH): $\varphi^3(x,y) = \varphi(x)\varphi(y)$

Thus the detail signal is contained in three sub images

$$w^1_{j+1}(k_x,k_y) = \sum_{lx=-\infty}^{+\infty}\sum_{ly=-\infty}^{+\infty} g(l_x)h(l_y)c_{j,k+2^j}(l_x,l_y) \quad (17)$$

$$w^2_{j+1}(k_x,k_y) = \sum_{lx=-\infty}^{+\infty}\sum_{ly=-\infty}^{+\infty} h(l_x)g(l_y)c_{j,k+2^j}(l_x,l_y) \quad (18)$$

$$w^3_{j+1}(k_x,k_y) = \sum_{lx=-\infty}^{+\infty}\sum_{ly=-\infty}^{+\infty} g(l_x)g(l_y)c_{j,k+2^j}(l_x,l_y) \quad (19)$$

3.5 Ridgelet Transform

In 1998, Donoho introduced the ridgelet transform. Continuous Rridgelet transform (CRT) can be defined from a 1D wavelet function oriented at constant lines and radial directions. Ridgelet transform has been generating a lot of interest due to its superior performance over wavelets, while wavelets have been very successful in applications such as denoising and compact approximations of images containing zero dimensional or point singularities. Wavelets do not isolate the smoothness along edges that occur in images, and they are thus more appropriate for the reconstruction of sharp point singularities than lines or edges. These shortcomings of wavelet are well addressed by the ridgelet transform; the functionality of wavelet has been extended to higher dimensional singularities and becomes an effective tool to perform sparse directional analysis. Generally speaking, wavelets detect objects with point singularities, while ridgelets are able to represent objects with line singularities.

The Finite Ridgelet Transform (FRIT) was computed in two steps: a calculation of discrete radon transform and an application of a wavelet transform. The Finite Radon Transform (FRAT) is computed in two steps: a calculation of 2D Fast Fourier Transform (FFT) for the image and an application of a 1D inverse Fast Fourier Transform (IFFT) on each of the 32 radial directions of the radon projection. 1D wavelet is applied restricted to radial directions going through the origin for three levels of decompositions. Applying FRAT on image can be presented as a set of projections of the image taken at different angles to map the image space to projection space. Its computation is important in image processing and computer vision for problems such as pattern recognition and the reconstruction of medical images. For discrete images, a projection is computed by summation of all data points that lie within specified unit-width strips; those lines are defined in a finite geometry.

The FRAT of a real function on the finite grid Z_p^2 is defined in

$$r_k[l] = \mathrm{FRAT}_f(k,l) = \frac{1}{\sqrt{P}} \sum_{(i,j)\in L(k,l)} f(i,j) \qquad (20)$$

In equation (20) the term L(k, l) denotes the set of points that make up a line on the lattice Z_p^2 as in

$$L(k,l) = \{(i,j): j = k_i + l(\mathrm{mod}\ p), i \in Z_p\} \qquad (21)$$

Where $0 \leq k < p$

$$L(k,l) = \{(i,j): j \in Z_p\} \qquad (22)$$

To compute the K^{th} radon projection (i.e., the K^{th} row in the array), all pixels of the original image need to be passed once and use P histogram's: one for every pixel in the row. At the end, all P histogrammed values are divided by K to get the average values. Each output of the radon projection is simply passed through the wavelet transform before it reaches the output multiplier. As shown in Figure 7, ridgelets use FRAT as a basic building block, where FRAT maps a line singularity into point singularity, and the wavelet transform has been used to effectively detect and segment the point singularity in radon domain.

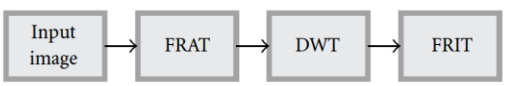

Figure 7. FRIT block diagram.

Ridgelet transformation on medical images was not promising. Medical images comprised of curves which are still not singularity points after applying radon transform. Wavelet transform cannot detect those singularities properly, since it is still not singularity points, resulting that ridgelet transformation is not suitable for de-noising these images. Ridgelet transform can be used in other applications, where images contain edges and straight lines. Figure 8 illustrates the radial grid in ridgelet transform; however, straight lines evaluate the image in the frequency domain.

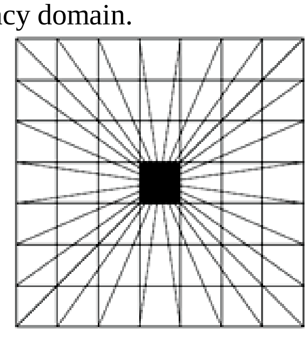

Figure 8. Ridgelet parameters.

4. IMAGE DENOISING

Image De-noising is used to produce good estimates of the original image from noisy observations. The restored image should contain less noise than the observations while still keep sharp transitions (i.e edges)

Suppose an image f(m,n) is corrupted by the additive noise

$g(m,n) = f(m,n) + \eta(m,n)$

where $\eta(m,n)$ are independent identically distributed Gaussian random variable with zero mean and variance σ^2. Image de-noising algorithms vary from simple thresholding to complicate model based methods. However simple thresholding methods can remove most of the noise.

4.1 Thresholding Function

The most frequently used thresholding methods are soft and hard thresholding. The soft thresholding ignores signals below noise threshold and attenuates low level signals. There is a smooth transition between on/off. The hard thresholding also ignores the signals below the noise threshold but there is sharp transition from on/off.

1. Soft Thresholding is defined by a fixed threshold σ

$$S_\sigma(x) = \begin{cases} x - \sigma & x \geq \sigma \\ 0 & |x| < \sigma \\ x + \sigma & x \leq \sigma \end{cases} \qquad (23)$$

2. Hard Thresholding

$$S_\sigma(x) = \begin{cases} x & |x| \geq \sigma \\ 0 & |x| < \sigma \end{cases} \qquad (24)$$

These thresholding functions might be a good choice because large coefficients remain nearly unaltered.

5. Bivariate Shrinkage function for Image De-noising

To model the statistics of wavelet coefficients of images, a new simple non-Gaussian bivariate probability distribution function is implemented in this paper. The model captures the dependence between a wavelet coefficient and its parent. Using Bayesian estimation theory, this model is derived, which generalizes the soft thresholding approach. The new shrinkage function, which depends on both the coefficient and its parent, yields improved results for wavelet based image denoising.

Let w_2 represent the parent of w_1. Then, y = w+n. Where $w = (w_1, w_2)$, $y = (y_1, y_2)$ and $n = (n_1, n_2)$. The noise values n_1, n_2 are zero mean Gaussian. Based on the empirical histograms, the non-Gaussian bivariate PDF is given by,

$$P_w(w) = \frac{3}{2\pi\sigma^2}\exp\left(-\frac{\sqrt{3}}{\sigma}\sqrt{w_1^2 + w_2^2}\right) \tag{25}$$

With this PDF, w_1 and w_2 are uncorrelated, but not independent. The MAP estimator of w_1 yields the following bivariate shrinkage function

$$\hat{w}_1 = \frac{\sqrt{y_1^2 + y_2^2} - \frac{\sqrt{3}\sigma_n^2}{\sigma}}{\sqrt{y_1^2 + y_2^2}}\, y_1 \tag{26}$$

For this bivariate shrinkage function, the smaller the parent value, the greater the shrinkage. This is consistent with other models, but here it is derived using a Bayesian estimation approach beginning with the new bivariate non-Gaussian model.

5.1 Denoising Algorithm:

1. Set the window size. The signal variance of a coefficient will be estimated using neighboring coefficients in a rectangular region with this window size.
2. Set number of stages to be used for the wavelet transforms.
3. Extend the noisy image. (The noisy image will be extended using symmetric extension in order to improve the boundary problem.)
4. Calculate the forward dual-tree DWT.
5. Estimate the noise variance. The noise variance will be calculated using the robust median estimator.
6. Process each sub band separately in a loop. First the real and imaginary parts of the coefficients and the corresponding parent matrices are prepared for each sub band.
7. Estimate the signal variance and the threshold value: (The signal variance for each coefficient is estimated using the window size and the threshold value for each coefficient will be calculated and stored in a matrix with the same size as the coefficient matrix.)
8. Estimate the magnitude of the complex coefficients. (The coefficients will be estimated using the magnitudes of the complex coefficient, its parent and the threshold value with the Bivariate Shrinkage Function.)
9. Calculate the inverse wavelet transform.
10. Extract the image. (The necessary part of the final image is extracted in order to reverse the symmetrical extension.)

5.2 Local Adaptive Image Enhancement

Using the bivariate shrinkage function shown in Equation (26),an effective and low complexity locally adaptive image denoising algorithm is proposed in this paper. This shrinkage function requires the prior knowledge of the noise variance and the signal variance for each wavelet coefficient Therefore the algorithm first estimates these parameters for the recipe of the estimation rules.

5.3Local Adaptive Algorithm

The estimator requires the prior knowledge of the noise variance σ_n^2 and the marginal variance σ^2 for each wavelet coefficient. In the algorithm, the marginal variance for the k^{th} coefficient will be estimated using neighboring coefficients in the region N(k). Here N(k) is defined as all coefficients with in a square-shaped window that is centered at the kth coefficient.

To estimate the noise variance σ_n^2 from the noisy wavelet coefficients, a robust median estimator is used from the finest scale wavelet co-efficient.

$$\hat{\sigma}_n^2 = \frac{\text{median}\,(|y_i|)}{0.6745},\, y_i \in \text{subband HH} \tag{27}$$

Let us assume we are trying to estimate the marginal variance σ^2 for the k^{th} wavelet coefficient. From the observation model, one gets $\sigma_y^2 = \sigma^2 = \sigma_n^2$ where σ_y^2 the marginal variance of the noisy observations y1 and y2 is. Since y1 and y2 are modeled as zero mean, σ_y^2 can be found empirically by

$$\hat{\sigma}_y^2 = \frac{1}{M}\sum_{y_i \in N(k)} {y_i}^2 \tag{28}$$

Where M is the size of the neighborhood N(k). Then σ can be estimated as

$$\hat{\sigma} = \sqrt{\hat{\sigma}_y^2 - \hat{\sigma}_n^2} \tag{29}$$

The algorithm is summarized as follows

(1) Calculate the noise variance $\hat{\sigma}_n^2$ using (27)

(2) For each wavelet coefficient (k=1 number of wavelet coefficients)

   (a) Calculate $\hat{\sigma}_y^2$ using (28)

   (b) Calculate $\hat{\sigma}$ using (29)

   (c) Estimate each coefficient using $\hat{\sigma}$ and $\hat{\sigma}_n^2$ using equation (26)

6 Experimental Results

Several experiments on simulated noise such as Random noise with a variance of σ = 20, Salt and Pepper noise with a variance of σ = 0.01 , Gaussian noise with a variance of 0.01, speckle noise with a variance of 0.02 and Poisson noise were performed to validate the image domain optimization method. The various noises are simulated by MATLAB Image Processing Tool Box. 8 bit biomedical images such as CT, MRI, X-Ray, PET and SPECT of size 256 x 256 were experimented.

The PSNR is used to compare the results quantitatively which can represent how smooth the de-noised image is. It is a quality measurement between the original and de-noised image. The higher the PSNR the better is the quality of the reconstructed image.

$$\mathrm{PSNR} = 10\log_{10}\left(\frac{f_{\max}^2}{\mathrm{MSE}}\right) \tag{30}$$

In equation (30) the term fmax is the maximum value of the image intensities and MSE is the Mean Square Error between the reconstructed image and original one

$$\mathrm{MSE} = \frac{1}{MN}\sum_{m=0}^{M-1}\sum_{n=0}^{N-1}\left|f(m,n) - \tilde{f}(m,n)\right|^2 \tag{31}$$

In equation (31) the term f(m,n) is the original image, the term $\tilde{f}(m,n)$ is the de-noised image and M x N is the number of pixels. The de-noised image is closer to the original one when PSNR is higher. The PSNR values were obtained for various bio-medical images and for each image type three samples were taken and the average PSNR of the noisy and de-noised images were calculated to ascertain the overall performance of the system in terms of average PSNR gain. Results presented in Tables 1 to 5 are in terms of average PSNR gain which demonstrate the effectiveness of a particular type of Wavelet technique applied to noisy versions of biomedical images like CT, MRI, X-ray, PET and SPECT .

Experiment 1

Experiments were conducted on five test images, CT,MRI,X-ray, PET and SPECT of size 256 x 256. Three samples of all these biomedical images were experimented. It is observed from Table 1 that the DTCWT outperforms other Wavelet techniques and Ridgelet for images corrupted by Random noise with noise variance of σ = 20.

Figure 9 shows the de-noising results of CT image implemented with DTCWT corrupted by random noise of variance =20.

Table 1: Denoising results (Average PSNR Gain in dB) for Random noise, Variance σ=20

Image	SWT (Hard Thresholding)	DWT with Bivariate shrinkage	Dual tree Complex Wavelet Transform	Ridgelet
CT	6.7345	8.0351	**9.1595**	0.2627
MRI	5.6436	7.5145	**8.2605**	0.3679
X-Ray	8.3341	9.2244	**10.4108**	0.5792
PET	8.0682	8.4313	**9.4574**	1.1541
SPECT	5.5048	7.3182	**8.3155**	-0.3708

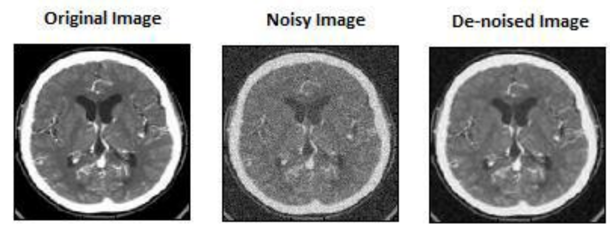

Figure 9: Denoising results of Dual Tree Complex Wavelet Transform for CT Image (Random Noise – variance = 20) (a) Original (b) Noisy (PSNR=21.6068 dB) (c) Recovered (PSNR = 31.1506dB)

Experiment 2

Simulations were carried out on five test images of size 256 x 256 and three samples in each were tested. The images were corrupted by Salt and Pepper noise with a noise variance of σ = 0.01. Table 2 illustrates that the DTCWT offers an excellent choice in the removal of Salt and Pepper noise in biomedical images. The results shown in Figure 10 is for MRI image denoised by DWT.

Table 2: Denoising results (Average PSNR Gain in dB) for Salt and Pepper noise, Variance = 0.01

Image	SWT (Hard Thresholding)	DWT with Bivariate shrinkage	Dual tree Complex Wavelet Transform	Ridgelet
CT	3.0687	3.0121	**3.0624**	-0.2844
MRI	3.0395	3.0167	**3.0434**	0.1301
X-Ray	3.0202	3.0114	**3.0349**	0.1614
PET	3.0159	3.0118	**3.0278**	1.0156
SPECT	3.0459	3.0162	**3.0810**	-0.7398

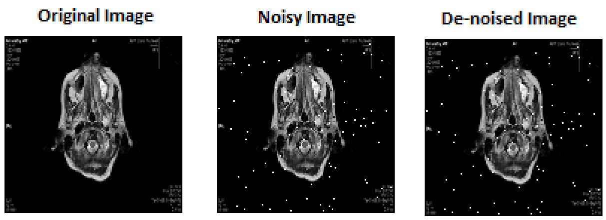

Figure 10: Denoising results of Discrete Wavelet Transform for MRI Image (Salt and Pepper Noise – variance = 0.01) (a) Original (b)Noisy (PSNR=20.5025) (c) Recovered (PSNR= 23.5130dB)

Experiment 3

Five types of biomedical images (i.e) CT, MRI, X-ray, PET and SPECT of size 256 x 256 are used for experimental evaluation purpose. The noise added is Gaussian noise with a noise variance of 0.01.Table 3 depicts that the DTCWT is a good choice for de-noising medical images degraded by Gaussian noise. The results are shown in Figure 11 for X-ray image denoised by DTCWT corrupted by Gaussian noise.

Table 3: Denoising results (Average PSNR Gain in dB) for Gaussian noise, Variance = 0.01

Image	SWT (Hard Thresholding)	DWT with Bivariate shrinkage	Dual tree Complex Wavelet Transform	Ridgelet
CT	6.3088	6.4182	**6.7490**	1.0821
MRI	5.1331	6.0494	**6.4693**	1.0546
X-Ray	7.4330	7.2125	**7.5920**	1.3010
PET	**6.0766**	5.7304	5.9040	1.5893
SPECT	5.3670	5.8314	**6.3114**	0.5065

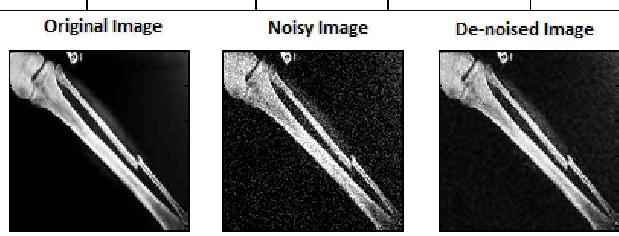

Figure 11: Denoising results of Dual Tree Complex Wavelet Transform for XRAY Image (Gaussian Noise – variance = 0.01) (a) Original (b)Noisy (PSNR=20.7678 dB) (c) Recovered (PSNR= 27.4066dB)

Experiment 4

The performance of the different Wavelet techniques and Ridgelets are demonstrated on five biomedical images of size 256 x 256 with three samples of each category viz, CT, MRI, X-ray, PET and SPECT. The noise added is Speckle noise with a variance of 0.02.

From Table 4 it is observed that the average PSNR gain is highest for almost all types of biomedical images with SWT (Stationary Wavelet Transform) using hard thresholding of Wavelet co-efficient. The results are shown in Figure 12 for PET image degraded by Speckle noise..

Table 4: Denoising results (Average PSNR Gain in dB) for Speckle noise, Variance = 0.02

Image	SWT (Hard Thresholding)	DWT with Bivariate shrinkage	Dual tree Complex Wavelet Transform	Ridgelet
CT	**4.6094**	3.5913	3.4980	-1.0242
MRI	**4.9711**	3.2757	3.3388	-2.8150
X-Ray	**3.6614**	3.1221	3.1624	-0.6306
PET	**3.1775**	3.0282	3.0484	-1.1298
SPECT	**3.9883**	3.1027	3.1879	-2.2094

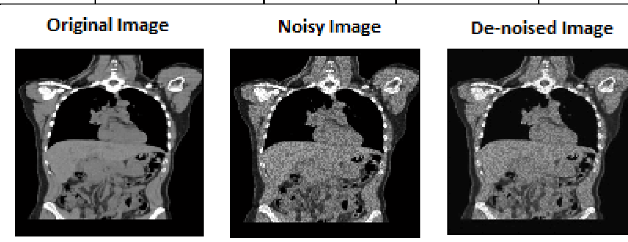

Figure 12: Denoising results of Stationary Wavelet Transform for PETA Image (Speckle Noise – variance=0.02) (a) Original (b) Noisy (PSNR=24.2552 dB) (c) Recovered (PSNR = 27.7610dB)

Experiment 5

8 bit biomedical images of dimension 256 x 256 are used for simulation. The image is corrupted by adding Poisson noise. It can be observed from Table 5 that the SWT (hard thresholding) outperforms other transforms in the removal of Poisson noise. The results are shown in Figure 13 for SPECT image degraded by Poisson noise with SWT.

Table 5: Denoising results (Average PSNR Gain in dB) for Poisson noise

Image	SWT (Hard Thresholding)	DWT with Bivariate shrinkage	Dual tree Complex Wavelet Transform	Ridgelet
CT	**4.3539**	3.5636	3.7874	-3.0568
MRI	3.4726	3.7377	**3.9504**	-4.3380
X-Ray	**5.1818**	3.5748	3.6526	-2.8401
PET	**3.2843**	3.0464	3.0828	-3.0471
SPECT	**4.5135**	3.2838	3.4074	-4.0974

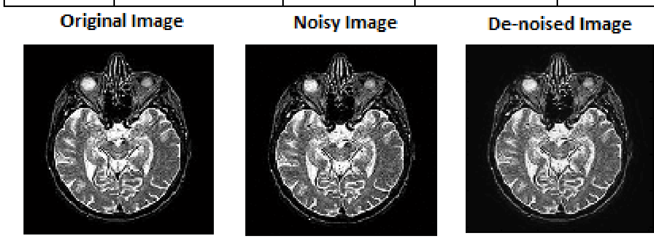

Figure 13: Denoising results of Stationary Wavelet Transform for SPECT Image (Poisson Noise) (a) Original (b) Noisy (PSNR=28.4781dB) (c) Recovered (PSNR = 31.6641dB)

Experiment6

In this experiment Ridgelets are used to denoise different biomedical images corrupted by various types of noise. Tables 1 to 5 clearly demonstrates that Ridgelets offers the lowest PSNR gain for all medical images and further the results as seen in Table 5 reveal that Ridgelets offers a negative average PSNR gain in the removal of Poisson noise in medical images. Figure 14 shows the results of X-ray image corrupted by Poisson noise with Ridgelets. The effectiveness of the Dual tree Complex Wavelet Transform is demonstrated in terms of average PSNR gain by comparing it with SWT, DWT and Ridgelets in the removal of random noise, Gaussian noise and Salt and Pepper noise. The comparison reveals that DTCWT offers the highest PSNR gain. The redundant SWT with hard thresholding is a better choice for the removal of Speckle noise and Poisson noise in medical images .Incorporation of Ridgelet transform is a poor choice for the removal of various types of noise in biomedical images as it shows a negative average PSNR gain and is ideally suitable to resolve straight line singularities.

Figure 14: Denoising results of Ridgelet Transform for X-ray Image (Poisson Noise) (a) Original (b) Noisy (PSNR=38.7250dB) (c) Recovered (PSNR = 35.9319dB)

The charts for comparison of de-noising various imaging modalities are depicted in Figures 15 to 19.

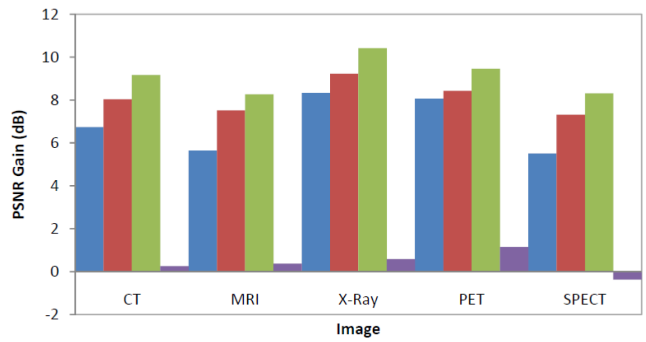

Figure 15: Chart for comparison of denoising performance of various imaging modalities with Random noise using multiresolution transforms

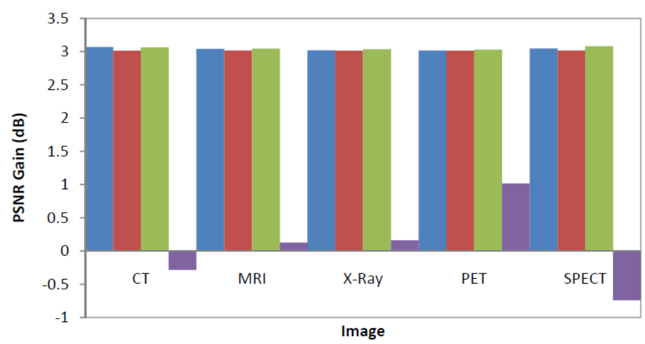

Figure 16: Chart for comparison of denoising performance of various imaging modalities with Salt and Pepper noise using multiresolution transforms

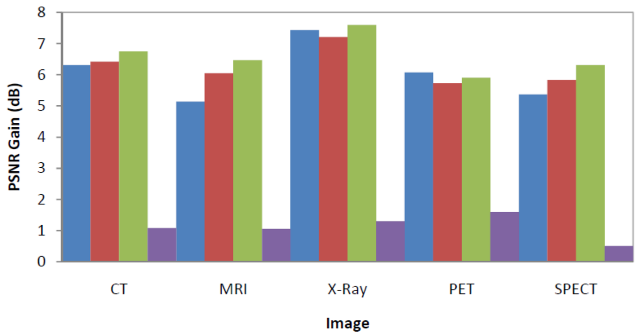

Figure 17: Chart for comparison of denoising performance of various imaging modalities with Gaussian noise using multiresolution transforms

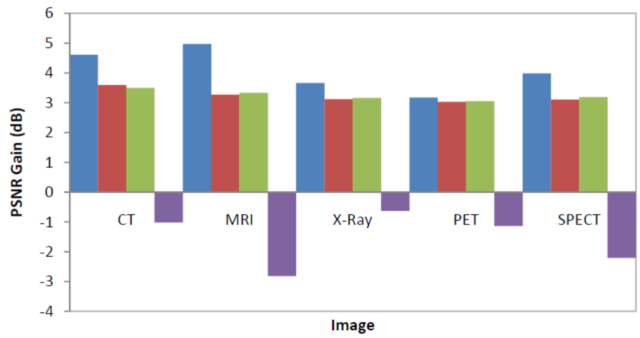

Figure 18: Chart for comparison of denoising performance of various imaging modalities with Speckle noise using multiresolution transforms

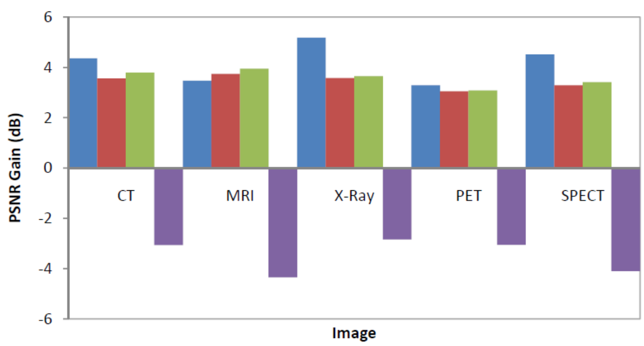

Figure 19: Chart for comparision of denoising performance of various imaging modalities with Poisson noise using multiresolution transforms

Legends on Charts:

SWT (Hard Thresholding)
DWT with Bivariate Shrinkage
Dual Tree Complex Wavelet Transform
Ridgelet

7 Conclusions

This paper investigates the comparative study of four techniques namely DWT(Bivariate shrinkage), SWT(hard thresholding), DTCWT(Bivariate shrinkage) and Ridgelet transform for de-noising of biomedical images degraded by different kinds of noise. The different image denoising methods are compared by the objective measure of performance, viz PSNR. The denoising algorithm is tested on biomedical images namely CT, MRI, X-ray, PET and SPECT with various noises added to the images. A very simple hard thresholding of coefficients is used with SWT and Ridgelet transform while bivariate shrinkage rule is used for DWT and DTCWT.

Local Adaptive de-noising methods in combination with bivariate shrinkage improves the de-noising results. This algorithm is used with DWT and DTCWT and a bivariate function is used. First the image is decomposed by the wavelet transform to obtain the approximation coefficients and detail coefficients in different sub bands. Then the bivariate shrinkage function is applied in order to characterize the dependencies between a co-efficient and a parent.

The DWT functions insufficiently in some of the image processing tasks due to strong shift dependence, lack of directional selectivity, aliasing and oscillations of the coefficients. The DTCWT due to its approximate shift invariance and improved directional selectivity outperforms the DWT in a wide range of applications. The comparison suggests that the DTCWT with bivariate shrinkage are competitive with other wavelet based techniques in the removal of Random noise, Gaussian noise and Salt and Pepper noise in biomedical images while the redundant SWT with hard thresholding seems to be a better choice for de-noising biomedical images degraded by speckle noise and Poisson noise.

It is also observed that Ridgelet transform offers a negative PSNR gain in de-noising biomedical images. This is due to the fact that Ridgelet transform can be used in applications where images contain edges and straight lines (i.e.) Ridgelet transform is effective in detecting linear radial structures which are not dominant in medical images. In future the work can be extended by using different types of noise variance also. Hence it is concluded that Ridgelet transform offers inferior results in de-noising all medical imaging modalities corrupted by various types of noise.

7 References

[1] R.R Coifman and D.L Donoho, " Translation Invariant De-noising",In Wavelets and Statistics, Springer Lecture notes in Statistics, Vol 103, Springer Verlag, New York pp 125-130.

[2] D.L.Donoho and I.M. Johnstone," Ideal Spatial adaptation by Wavelet shrinkage", Biometrika,81:425-455,March 1994.

[3] D.L.Donoho,"De-noising by soft thresholding", Technical report 409, department of Statistics Stanford University,1995.

[4] N.G. Kingsbury, " The Dual tree Complex wavelet Transform: A new efficient tool for image restoration and enhancement", Proc EUSIPCO'98 Rhodes, pp 319-322, 1998.

[5] Levent Sendur and Ivan W. Selesnik, " Bivariate shrinkage with Local Variance Estimation", IEEE Signal Processing Letters Vol 9, No 12, Dec 2002.

[6] M. Do. Vetterli," The Finite Ridgelet Transform for Image representation", IEEE Transactions on Image Processing 12(1) ,2003,16-28

[7] X. H. Wang, Robert S. H. Istepanian,"Microarray Image Enhancement for De-noising using Stationary Wavelet Transform", IEEE Transactions on Nanobioscience, vol2,No 3, December 2003.

[8] R.Gomathi and S. Selvakumaran," A Bivariate shrinkage function for Complex Dual tree based Image de-noising", Proceedings of the 6th WSEAS International Conference on Wavelet Analysis and Multirate Systems, Oct 16-18, 2006.

[9] Ling Wang, Jianming Lu, Yeqiu Li, Takashi Yahagi," Noise removal for Medical X-ray images in Multiwavelet domain",International Symposium on Intelligent Signal Processing and Communication Systems ,2006.

[10] Latha Parthiban, R. Subramanian," Speckle Noise removal using Contourlets", 2006 IEEE

[11] Shuai Xing, Qing Xu," Speckle De-noising based on Bivariate shrinkage function and Dual tree Complex Wavelet Transform",The International Archives of the Photogrammetry, remote Sensing and Spatial Information Sciences, Vol XXVII, Beijing 2008.

[12] Mark Miller, Nick Kingsbury," Image De-noising using Derotated Complex Wavelet Co-efficients", IEEE Transactions on image Processing, Vol 17, No 9, September 2008.

[13] Syam Lal, Mahesh Chandra and Gopal Krishna Upadhyay," Noise removal algorithm for images corrupted by additive Gaussian noise", International Journal of Recent trends in Engineering Vol 2, No 1, Nov 2009.

[14] Wen-Chien Yen, Shen-Chuan Tai," Dual Tree Wavelet based Algorithm for Speckle reduction and Edge Enhancement in Ultrasound Images", 2010 3rd International Conference on Biomedical Engineering and Informatics.

[15] Shan Gai, Peng Liu etal., " A new Image De-noising Algorithm via Bivariate Shrinkage based on Quarternion Wavelet Transform", Journal of Computational Information Systems 6:11(2010) 3751-3760.

[16] Gornale S.S et al," Finger Print image De-noising using multiresolution Analysis(MRA) through Stationary wavelet Transform method", International Journal of Knowledge Engineering, Vol1, Issue1, 2010 pp 05-14

[17] Ioana Firoiu, Alexandru ISAR, Dorina ISAR," A Bayesian Approach of Wavelet based image denoising in a Hyper Analytic Multiwavelet context", WSEAS Transactions on Signal Processing, Issue 4, Vol 6, October 2010.

[18] D. Mary Sugantharathnam,Dr. D. Manimegalai," The Curvelet Approach for De-noising in various Imaging Modalities using different shrinkage rules",IJCA, Vol 29-No 7 , Sept 2011.

[19] S. Kother Mohideen," Denoising of Images using Complex Wavelet Transform", International Journal of Advanced Scientific Research and Technology, Issue 2, Vol1, Feb 2012.

[20] V. Naga Prudhviraj, Dr. T. Venkateswarlu," De-noising of Medical Images using undecimated wavelet Transform", Recent Advances in Intelligent Computational Systems (RAICS), 2011 IEEE, 483 – 488, Sept., 2011.

[21] H.A.Noubari, A.Fayazi & F.Babapoui,"De-noising of SPECT images via Optimal thresholding by Wavelets, 31st Annual Conference of the IEEE EMBS.

[22] Bahendwar. Y and Sinha G.R(2012) ," A modified Algorithm for denoising MRI images of Lungs using Discrete Wavelet Transform",IJCA proceedings on National Conference on Innovative Paradigms in

Engineering and Technology(NCIPET 2012), NCIPET(1):29-32 March 2012.

[23] F.Neri," A Comparative Study of Financial Agent Simulator Across Learning Scenarios", Agents and Data Mining Interaction, Lecture Notes in Computer Science 7103, Springer Berlin,2012,pp. 86-97.

[24] C. Avilés-Cruz, A. Ferreyra-Ramirez, J. J. Ocampo-Hidalgo, I. Vazquez-Alvarez, "Structured - Image Retrieval invariant to rotation, scaling and Translation", WSEAS TRANSACTIONS on SYSTEMS, Issue 8, Volume 8, August 2009.

[25] Jiann-Shiou Yang, "Estimation of Vehicle's Lateral Position via the Lucas-Kanade Optical Flow Method", WSEAS TRANSACTIONS on SYSTEMS, Issue 8, Volume 11, August 2012.

[26] Hum Yan Chai, Lai Khin Wee, Tan Tian Swee, Sheikh Hussain, "Gray-Level Co-occurrence Matrix Bone Fracture Detection", WSEAS TRANSACTIONS on SYSTEMS, Issue 1, Volume 10, January 2011.